

Premature Truncation of a Novel Protein, RD3, Exhibiting Subnuclear Localization Is Associated with Retinal Degeneration

James S. Friedman, Bo Chang, Chitra Kannabiran, Christina Chakarova, Hardeep P. Singh, Subhadra Jalali, Norman L. Hawes, Kari Branham, Mohammad Othman, Elena Filippova, Debra A. Thompson, Andrew R. Webster, Sten Andréasson, Samuel G. Jacobson, Shomi S. Bhattacharya, John R. Heckenlively, and Anand Swaroop

The *rd3* mouse is one of the oldest identified models of early-onset retinal degeneration. Using the positional candidate approach, we have identified a C→T substitution in a novel gene, *Rd3*, that encodes an evolutionarily conserved protein of 195 amino acids. The *rd3* mutation results in a predicted stop codon after residue 106. This change is observed in four *rd3* lines derived from the original collected mice but not in the nine wild-type mouse strains that were examined. *Rd3* is preferentially expressed in the retina and exhibits increasing expression through early postnatal development. In transiently transfected COS-1 cells, the RD3-fusion protein shows subnuclear localization adjacent to promyelocytic leukemia-gene-product bodies. The truncated mutant RD3 protein is detectable in COS-1 cells but appears to get degraded rapidly. To explore potential association of the human *RD3* gene at chromosome 1q32 with retinopathies, we performed a mutation screen of 881 probands from North America, India, and Europe. In addition to several alterations of uncertain significance, we identified a homozygous alteration in the invariant G nucleotide of the *RD3* exon 2 donor splice site in two siblings with Leber congenital amaurosis. This mutation is predicted to result in premature truncation of the RD3 protein, segregates with the disease, and is not detected in 121 ethnically matched control individuals. We suggest that the retinopathy-associated RD3 protein is part of subnuclear protein complexes involved in diverse processes, such as transcription and splicing.

Retinitis pigmentosa (RP [MIM #268000]) encompasses a group of retinal degenerative diseases (RDs) that severely compromise the quality of life of affected individuals. RP is genetically heterogeneous, with mutations in multiple genes; to date, 168 retinal-disease loci have been mapped, and 117 retinal disease-associated genes have been identified (RetNet Web site).¹ A majority of RP-causing genes encode proteins involved in phototransduction, photoreceptor morphogenesis, trafficking, gene regulation, and/or splicing.² Mutations in some of the genes are suggested to cause a prolonged and/or increased phototransduction, followed by decreased Ca⁺⁺ levels, leading to photoreceptor-cell death.³ Despite major advances, genetic defects have not been determined for a significant proportion of subjects with RP (RetNet Web site).⁴⁻⁶

One approach for identification of additional human retinopathy genes is to elucidate the molecular basis of retinal degeneration in animal models. At least 35 strains of mice exhibit retinal degenerative disease.^{7,8} Some examples of retinal degeneration (rd) mice include *rd1* (*Pde6b*), *Rds* (*peripherin*), *rd7* (*Nr2e3*), and *rd16* (*Cep290/NPHP6*), and their known and putative biological functions closely correspond to genes involved in human retinal disease.⁹⁻¹³

Mutations in their human orthologs are associated with retinopathies.¹⁴⁻¹⁸

The retinal degeneration 3 (*rd3*) mice were originally collected in Switzerland in 1969, were sent to the Jackson Laboratory, were bred as different lines to establish their Robertsonian translocation, and were later identified as having retinal degeneration.¹⁹ Different strains of *rd3* have variable phenotypes, with photoreceptors starting to degenerate at age 2–3 wk and complete loss of photoreceptors at age 8–16 wk.¹⁹ Electroretinography (ERG) studies have demonstrated that the loss of retinal response was dependent on the genetic background, with ERGs becoming extinguished at age 6–16 wk in some strains.¹⁹ Hence, at least one modifier locus appears to slow down the rate of degeneration in the pigmented mice compared with the albino mice. A detailed morphological examination of three *rd3* strains demonstrated the degeneration of photoreceptors through apoptosis and has confirmed the slower rate of degeneration in pigmented *rd3* mice compared with albino strains.²⁰

The *rd3* genetic locus was mapped to mouse chromosome 1 between markers *D1Mit292* and *D1Mit510* and was excluded as being a mouse ortholog of one of the human

From the Departments of Ophthalmology and Visual Sciences (J.S.F.; K.B.; M.O.; E.F.; D.A.T.; J.R.H. A.S.) and Human Genetics (A.S.), W. K. Kellogg Eye Center, University of Michigan, Ann Arbor; the Jackson Laboratory, Bar Harbor, Maine (B.C.; N.L.H.); Kallam Anji Reddy Molecular Genetics Laboratory (C.K.; H.P.S.) and Kannuri Santhamma Retina-Vitreous Services (S.J.), L. V. Prasad Eye Institute, Banjara Hills, Hyderabad, India; Department of Molecular Genetics, Institute of Ophthalmology, University College London (C.C.; A.R.W.; S.S.B.), and Moorfield Eye Hospital (A.R.W.), London; Department of Ophthalmology, University Hospital of Lund, Lund, Sweden (S.A.); and Department of Ophthalmology, Scheie Eye Institute, University of Pennsylvania, Philadelphia (S.G.J.)

Received August 21, 2006; accepted for publication October 6, 2006; electronically published October 23, 2006.

Address for correspondence and reprints: Dr. Anand Swaroop, W. K. Kellogg Eye Center, University of Michigan, 1000 Wall Street, Ann Arbor, MI 48105. E-mail: swaroop@umich.edu

Am. J. Hum. Genet. 2006;79:1059–1070. © 2006 by The American Society of Human Genetics. All rights reserved. 0002-9297/2006/7906-0008\$15.00

Usher syndrome loci.^{21,22} Herein, we report the identification of the genes (*3322402L07Rik* and *C1orf36*—renamed “*Rd3*” and “*RD3*,” respectively) responsible for the *rd3* retinopathy. We show that *Rd3* is preferentially expressed in the retina and that the *rd3* mutation leads to a truncated and relatively unstable protein in COS-1 cells. The RD3 protein is associated with promyelocytic leukemia-gene-product (PML) bodies in the nucleus. We also describe a large *RD3*-screening effort involving 881 probands with retinopathy, revealing at least one putative disease-causing mutation and several changes of uncertain significance.

Material and Methods

Histological and Electroretinogram Analysis of rd3 Mice

The studies involving mice were performed after approval from institutional committees was obtained. Histology and electroretinograms were performed as described elsewhere.²³

Mouse Mutation Screen

We examined genes in the published *rd3* (RBF/DnJ) critical region by direct sequencing. We additionally screened other *rd3* lines (RBJ/DnJ, STOCK Rb(11.13)4Bnr/J, and STOCK In(5)30Rk/J), as well as wild-type (WT) mouse strains, to verify the alteration. The following primers were used: for *Rd3* exon 2, 5'-cgctctctcttctgtg-3' (forward) and 5'-gcgactccagtcacctctc-3' (reverse); for *Rd3* exon 3 5'-caagagcaaggtggaggt-3' (forward) and 5'-tccagcattcaaggactcag-3' (reverse). Exon amplification and sequencing of another gene, *Rcor3*, was initiated but was halted when the stop codon in *3322402L07Rik* was identified. PCR was performed from mouse-tail DNA with use of standard conditions, and amplified products were evaluated by agarose gel electrophoresis and were sequenced at the University of Michigan sequencing core facility.

RT-PCR and Northern-Blot Analysis

RT-PCR analysis was performed using WT mouse retinal RNA at time points ranging from embryonic day 12 (E12) to age 4 mo and from postnatal day 2 (P2) and 4-wk-old (4W) adult *Nrl*^{-/-} and *Crx*^{-/-} mice.^{24,25} The primers used were Hprt 5'-caacttgccttcctggt-3' (forward), Hprt 5'-caagggcatccaacaaca-3' (reverse), *Rd3rt* 5'-gagagagtgaggagcacaac-3' (forward), and *Rd3rt* 5'-cacatcctccgagatggttc-3' (reverse). A human multiple-tissue northern blot (BD Biosciences Clontech) and a mouse retina northern blot were probed with radiolabeled full-length *Rd3* cDNA or β -actin cDNA, as described elsewhere.²⁶

Immunoblot Analysis

Rd3 cDNA was amplified and cloned into the pEGFPN1 vector (BD Biosciences Clontech) with use of primers N1 5'-gagcagaagcttatagtgccctgaaggaggt-3' (forward) and N1 5'-cagcaggatccgagtcggcctggggcgccctgaa-3' (reverse). Mutagenesis was performed, as described elsewhere,²⁷ with primers W6R 5'-atgtccctcatcccggctcgggtggaagc-3' (forward), W6R 5'-cgttcaccggagccgaggatgaggacat-3' (reverse), E23D 5'-cggaccggccgacatggtctggagacg-3' (forward), E23D 5'-cgtctccagcaccatgctcggcggggctcg-3' (reverse), K130M 5'-gccctggagaagatgatcaggaggaggagcc-3' (forward), and K130M 5'-ggcctcctctctcgcacatcttctccagggc-3' (reverse). Primers used to transfer *Rd3* into pcDNA4c (Invitrogen) were *Rd3pc* 5'-gagcagcatcatgtccctcctccgtgg-3' (forward) and *Rd3pc* 5'-cagcaggcggcccttgatgggtc-

tcctgggtg-3' (reverse). Primers (*Rd3mut* 5'-gctgctggctgaatgagagcccgaggtg-3' [forward] and *Rd3mut* 5'-cacctcgggtctcattcagccagcagc-3' [reverse]) were used to introduce the *rd3* mutation into the mouse *Rd3* cDNA. The *rd3* cDNA construct was then used as a PCR template with *Rd3pcF* and *Rd3pcR* primers. The amplified PCR product was digested and cloned into pcDNA4. Each *Rd3* mutant cDNA clone was completely sequenced. Mouse *Mef2c* in pcDNA4 was used as a transfection control in some experiments. Expression constructs were transfected into COS-1 cells with FuGene 6 (Roche), according to the manufacturer's instructions. Cells were harvested after 48 h, with use of PBS and protease inhibitors (Roche), and extracts were fractionated by SDS-PAGE and were transferred to nitrocellulose membrane. The blots were probed with rabbit anti-Green Fluorescent Protein (GFP) polyclonal antibody (1:2,000) and mouse anti-beta tubulin antibody (1:10,000) or with mouse-anti Xpress antibody (1:4,000) (Invitrogen) and were visualized using appropriate secondary antibodies and luminescence (Pierce).

Localization in COS-1 Cells

Cells were washed with PBS 48 h after transfection, were fixed using 4% paraformaldehyde/PBS for 15 min, and were washed again in PBS. Cells were permeabilized using 0.05% Triton X-100/PBS (PBS-T) for 10 min. After washing, a 5% BSA/PBS solution was applied, and the cells were blocked for 30 min. The primary antibodies used were anti-coilin antibody ab11822 (1:50) (Abcam), anti-SC-35 antibody ab11826 (1:50) (Abcam), anti-PML antibody sc-5621 (1:50) (Santa Cruz Biotechnology), and anti-Xpress antibody (1:400) (Invitrogen). The cells were incubated for 1 h in 1% BSA/PBS with primary antibody, were washed with 1% BSA/PBS, and were incubated with the appropriate secondary: anti-rabbit IgG Alexa fluor 546, anti-mouse IgG Alexa fluor 546, or anti-mouse IgG Alexa fluor 488 (Molecular Probes) (1:750 dilution). Cells were washed with 1% BSA/PBS, were counterstained with bisbenzimidazole to stain nuclei, and were examined by fluorescent microscopy.

Human-Mutation Screen

All human studies were performed in a manner consistent with the Declaration of Helsinki and were approved by the respective institutional review boards. Appropriate informed consent was obtained from study subjects. We performed a three-continent (North America, Asia [India], and Europe [United Kingdom and Scandinavia]) human-mutation screen of the *RD3* gene. Clinical phenotypes observed among the North American patient pool included simplex RP, multiplex RP, juvenile (early-onset) RP, recessive RP, cone-rod dystrophy (CRD), Leber congenital amaurosis (LCA [MIM #204000]), partial cone degeneration, fundus albipunctatus, atypical pattern dystrophy, macular degeneration, Stargardt disease, autoimmune retinopathy, achromatopsia, congenital stationary night blindness, and enhanced S-cone syndrome. For the North American and European screen, the following primers were used: for exon 2, *RD3* 5'-ctgttagggcagagcaggtc (forward) and *RD3* 5'-ctctagtctggtggcctca (reverse); for exon 3, *RD3* 5'-ggactaattggccatgagga (forward) and *RD3* 5'-ctttgtggccagaggaag (reverse). The screen in India used exon 2 5'-ttccagggttccactctg-3' (forward) and 5'-ccactgcagccacttctc-3' (reverse) and exon 3 5'-gagccgggggtccagac-3' (forward) and 5'-gttccaggccggcgct-3' (reverse). PCR was performed using standard conditions, and products were subjected to direct sequencing. Sequencing

was performed at the University of Michigan sequencing core, at Bangalore Genei (Bangalore, India), and at the Institute of Ophthalmology (London). We performed RFLP analysis to determine segregation of a splice-site change within the LCA-affected family and to examine 121 unrelated ethnically matched unaffected controls. This change leads to the abolition of a restriction site for *Hph*1. The normal allele in a 436-bp amplified PCR product is digested into 387 bp and 49 bp fragments, whereas the homozygous mutated allele shows a 436-bp product.

Results

rd3 Mouse Strains and Visual-Function Analysis

The *rd3* mutation has been bred into different strains of mice and now exists in five separate strains—RBF/DnJ, STOCK In(1)Rk/J, STOCK In(5)30Rk/J, RBJ/DnJ, and STOCK Rb(11.13)4Bnr/J (hereafter termed “4Bnr”). An updated pedigree of *rd3*-bearing mice is shown in figure 1.¹⁹ Histologically, STOCK In(5)30Rk/J mice have a modest reduction in outer nuclear layer (ONL) thickness, with 3–5 rows of nuclei left at age 35 d. In contrast, the RBF/DnJ albino strain has a fully degenerated retina at the same age. The 4Bnr albino strain had the least degenerate retina of the three assessed *rd3/rd3* mice, but some degeneration was observed at the earlier time point of 27 d (fig. 2A).

For comprehensive evaluation of rod and/or cone photoreceptor dysfunction, we performed dark-adapted (rod photoreceptor derived) and light-adapted (cone photoreceptor derived) ERG tests on STOCK In(5)30Rk/J, 4Bnr, and RBF/DnJ *rd3/rd3* strains, with C57BL/6J mice as controls. In a previous study, rod derived ERG showed progressive retinal functional loss in *rd3* mice; no cone ERG was reported.^{19,28} We found that the amplitude of the loss of dark-adapted ERG varied, depending on the mouse strain. The In(5)30Rk/J (pigmented) strain had dark-adapted ERG closer to the WT at both age 24 d and age 32 d. The 4Bnr (albino) strain had a large response at day

17, but ERG was reduced at day 24. Lastly, the ERG in the RBF/DnJ (albino) strain was almost undetectable at age 24 d and was completely abolished by age 31 d (fig. 2B, top panel). All three strains of *rd3/rd3* mice had greatly reduced or nondetectable light-adapted ERGs by age 24 d (fig. 2B, bottom panel, and data not shown). These results demonstrate that both rod and cone photoreceptors in the *rd3* homozygotes are functionally affected.

Mutation Screen of *rd3* Mice

To identify the *rd3* mutation, we screened candidate genes in the mapped *rd3* region (fig. 3A) that had been defined elsewhere.²¹ The critical genomic region was ~1 Mb and contained 13 genes or expressed sequences (National Center for Biotechnology Information [NCBI] Map Viewer build 36.1). To select candidates for mutation analysis, we first examined the expression profile of all genes *in silico* and through our microarray profiling, as reported elsewhere.²⁹ The Riken cDNA 3322402L07 showed a twofold increase in expression from P2 to P10 in purified rod photoreceptors²⁹ (A. Swaroop, M. Akimoto, and H. Cheng, unpublished data). Hence, we selected it as a candidate gene for the *rd3* mutation screen. Complete sequencing of all exons and intron-exon boundaries (fig. 3B) revealed a homozygous c.319C→T transition in the third exon. This change alters codon 107 from CGA to TGA, thus converting arginine to a stop codon, and is predicted to result in premature truncation of the RD3 protein. The mutation was detected in all *rd3* lines tested (RBF/DnJ, RBJ/DnJ, 4Bnr, and STOCK In(5)30Rk/J) but not in the nine control WT mouse lines (C57BL/6J, A/J, AE/J, BALB/cJ, C3H/HeJ, CBA/J, DBA/2J, MOLC/RkJ, and NON/LtJ) (fig. 3C). To further confirm whether this is indeed the causative mutation in *rd3*-containing strains, we generated haplotypes using markers spanning the *rd3* locus.²¹ The three markers—

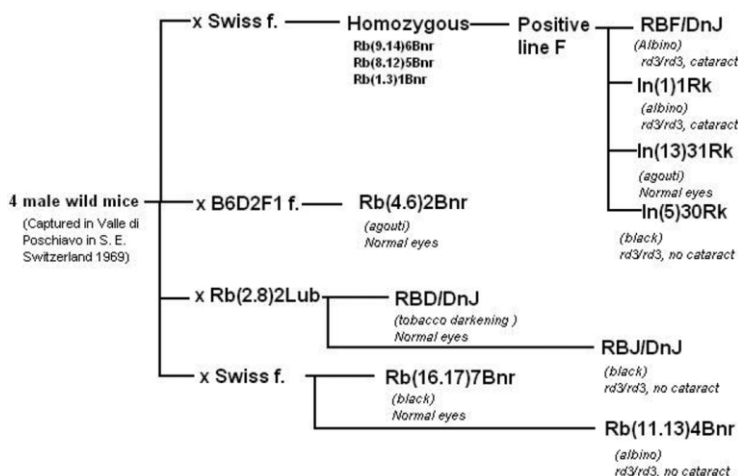


Figure 1. Pedigree of the *rd3* mouse strains. Four male mice were collected in Switzerland in 1969 and were genetically fixed to several lines. The mouse strains are currently housed at the Jackson Laboratory. This pedigree was updated from an earlier version,¹⁹ with the kind permission of Springer Science and Business Media.

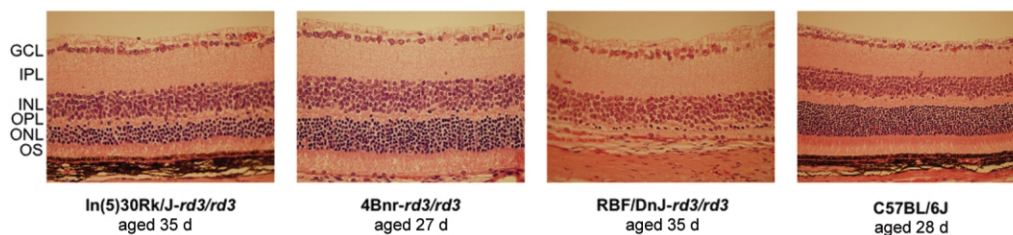
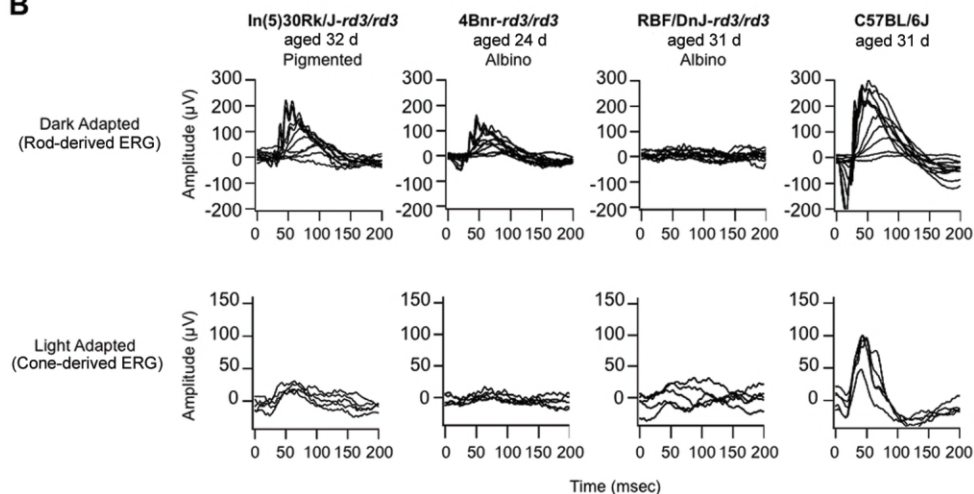
A**B**

Figure 2. *A*, Histology of *rd3/rd3* mice. We examined STOCK In(5)30Rk/J, 4Bnr, RBF/DnJ (all *rd3/rd3*), and control C57BL/6J mice at ages 35, 27, 35, and 28 d, respectively. *B*, *top*, ERG responses under dark-adapted conditions: STOCK In(5)30Rk/J(*rd3/rd3*) mice (aged 32 d), 4Bnr(*rd3/rd3*) mice (aged 24 d), RBF/DnJ(*rd3/rd3*) mice (aged 31 d), C57BL/6J mice (aged 31 d). *Bottom*, Light-adapted ERG responses of the same mice.

D1Mit292.1, *D1Mit462.2*, and *D1Mit511*—revealed identical alleles in the three tested *rd3* lines (data not shown), which is consistent with the presence of the *rd3* mutation in this genetic background.

Analysis of the *Rd3* Gene

To determine the expression profile of the *Rd3* transcript, we performed northern-blot and RT-PCR analysis using RNA from human and mouse tissues. The *Rd3* transcript of 1.9 kb was enriched in adult-mouse retinal tissues and had no detectable expression in nonretinal adult-human tissues, as revealed by human multiple-tissue northern-blot analysis (data not shown). We then examined its expression using WT, *Nrl*^{+/-}, and *Nrl*^{-/-} mouse retinal RNA by northern-blot analysis. WT mice and *Nrl*^{+/-} mice have a rod/photoreceptor-dominated retina, whereas *Nrl*^{-/-} mice lack rods and instead have a cone-dominant retina.²⁴ *Rd3* is transcribed as a single RNA in these strains, with no obvious difference (data not shown).

To elucidate developmental expression of *Rd3*, we performed RT-PCR experiments using mouse retinal RNA from

E12 to age 4 mo (fig. 4A). The *Rd3* transcript is detected at very low levels at E12 but was more noticeable beginning at E18, with subsequent increase in expression at P2 and P6. After P6, the levels of *Rd3* transcript remained high. Additional RT-PCR experiments were performed using retinal RNA from *Nrl*^{-/-} (aged P2 and 4W), *Crx*^{-/-} (aged P2 and 4W), *rd1* (adult), and *rd16* (adult) mice. The *Nrl*^{-/-} mouse lacks rod photoreceptors, whereas the *Crx*^{-/-} mouse exhibits a lessening of rod and cone gene expression at P10 and exhibits photoreceptor degeneration at age 2 mo.^{24,25} The *rd1* and *rd16* homozygotes exhibit early-onset degeneration of photoreceptors.^{9,13} The detection of the *Rd3* transcript in all mutant mouse strains suggests that it is also expressed in inner retina cell types (fig. 4B). Our data are consistent with the expression profile for C1orf36 (Hs.632495 [NCBI Expression Profile Viewer]) and previous in situ hybridization experiments,^{30,31} which demonstrate high expression of *3322402L07Rik* cDNA in the ONL in addition to the other cellular layers of the retina.

Clustal analysis of the RD3 protein orthologs suggests its strong conservation in vertebrates, from human to ze-

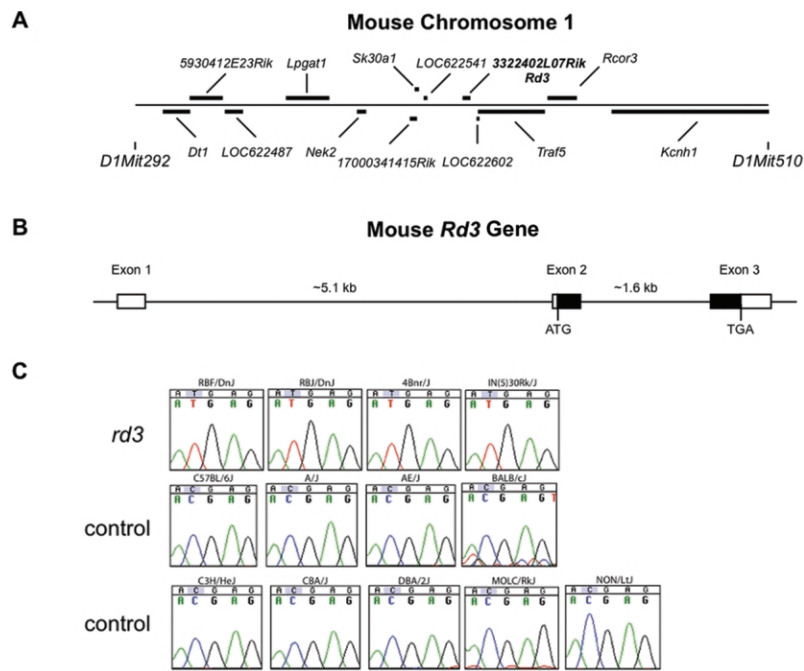


Figure 3. *A*, Critical genomic region encompassing the *rd3* mutation, between markers *D1Mit292* and *D1Mit510*.²¹ Genes within the critical region are indicated. *B*, Genomic structure of the mouse *Rd3* gene. *C*, Chromatogram showing the region of the *Rd3* (*3322402L07Rik*) molecular defect in *rd3/rd3* strains RBF/DnJ, RBJ/DnJ, STOCK Rb(11.13)4Bnr/J, STOCK In(5)30Rk/J, and WT control strains C57BL/6J, A/J, AE/J, BALB/cJ, C3H/HeJ, CBA/J, DBA/2J, MOLC/RkJ, and NON/LtJ. The homozygous C→T change in the *rd3*-bearing mice is indicated. It generates a stop codon after aa 106.

brafish (fig. 4C). An *in silico* analysis of the mouse and human RD3 proteins reveals a coiled-coil domain at aa 22–54 and another weaker coiled-coil domain at aa 121–141.³² The RD3 protein also has several putative protein kinase C and consensus Casein kinase II phosphorylation sites and one predicted sumoylation site. The mouse and human RD3 orthologs are basic proteins, with isoelectric points of 8.9 and 7.7, respectively.

Immunoblot analysis of COS-1 cells transfected with an *Rd3*-expression construct in the EGFPN1 vector demonstrated an expected RD3-GFP-fusion protein of ~45 kDa (predicted molecular mass of RD3 is ~22 kDa and that of GFP is ~23 kDa) (fig. 4D).

Localization of the RD3 Protein in Transfected COS-1 Cells

In transfected COS-1 cells, the RD3-GFP-fusion protein primarily exhibited nuclear or nuclear/cytoplasmic localization (fig. 5A–5D and data not shown). Some cells also contained a putative aggresome-like staining adjacent to the nucleus—likely because of the overexpression of the RD3 protein (data not shown). The most striking pattern was the presence of subnuclear spots, henceforth named “RD3 bodies,” of different sizes (fig. 5A–5C). We examined whether RD3 bodies colocalized with other subnuclear proteins, such as coilin (Cajal body marker), SC-35 (Nuclear Speckle marker), and promyelocytic leukemia gene product (PML body marker). Coilin staining did not lo-

calize near RD3 bodies in a consistent manner, suggesting that they are not associated (fig. 5A). SC-35 staining tended to be diffuse and localized near RD3 bodies (fig. 5B). PML staining also existed near RD3 bodies, with an occasional overlap (fig. 5C and 5G). To further confirm close PML proximity, we performed the same experiment using an Xpress-tagged *Rd3* plasmid. The Xpress-RD3 protein demonstrated a more highly varied localization pattern than did RD3-GFP, suggesting that the size of the tag may impact the distribution of transfected RD3 protein (fig. 5E and 5F). Nonetheless, we observed many cells with similar RD3 bodies in close proximity to PML bodies in Xpress-*Rd3*-transfected cells (fig. 5E and 5H).

Analysis of the *rd3* Mutation

To determine the consequence of the *rd3* mutation, we introduced this sequence alteration into the *Rd3*-pcDNA4 construct. Immunoblot analysis of COS-1-transfected cells revealed a truncated mutant RD3 protein (~11 kDa + ~4 kDa Xpress epitope), which was consistently detected at reduced levels compared with the WT protein (~22 kDa + ~4 kDa Xpress epitope) (fig. 6A). The mutant truncated protein therefore appears to be unstable and prematurely degraded. The mouse *Mef2c*-pcDNA4 construct was used as an internal control for transfection and was detected in roughly equal amounts in all experiments (fig. 6A). By immunocytochemistry, Xpress-RD3 mutant protein could

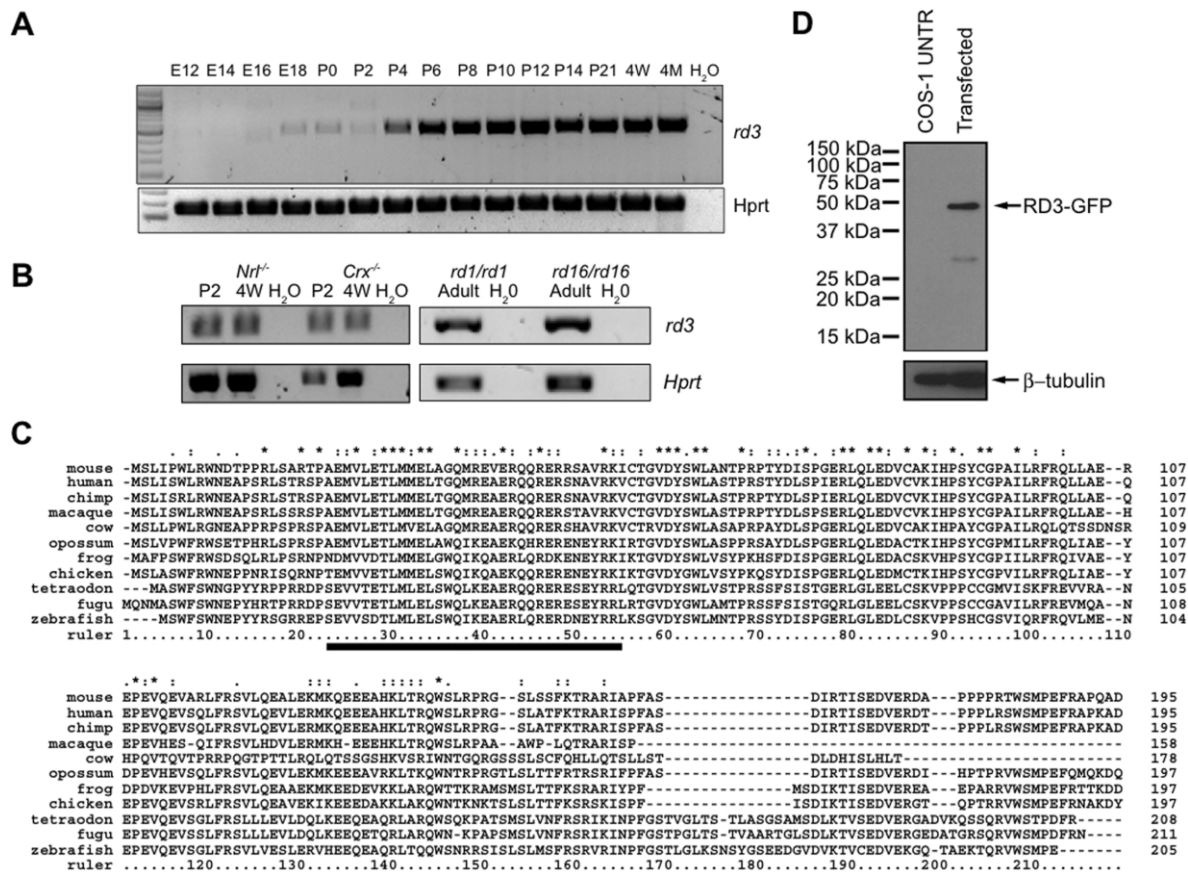


Figure 4. Expression of the *Rd3* gene. *A*, *Rd3* transcripts in mouse retina (aged E12 to 4 mo), present from at least E18, with a large increase from age P2 to age P6. *Hprt* was used to evaluate RNA quality and to normalize for quantity. *B*, Expression of *Rd3* in *Nrl*^{-/-}, *Crx*^{-/-}, *rd1/rd1*, and *rd16/rd16* mouse retina cDNA from P2, 4W, or adult. *Hprt* was used as a positive control. *C*, Alignment of RD3 protein orthologs. The amino acid sequence of mouse RD3 protein is aligned with those of human, chimpanzee, macaque, cow, opossum, frog, chicken, tetraodon, fugu, and zebrafish. Amino acid residues conserved in all orthologs are indicated by an asterisk (*), and reduced identity is shown using either a colon (:), or a dot (.). The long bar denotes a highly conserved coiled-coiled domain. *D*, Immunoblot expression of RD3-GFP fusion protein. An expression construct containing *Rd3*-GFP cDNA was transfected into COS-1 cells and was examined by immunoblot with use of anti-GFP antibody. The observed band is approximately the size estimated for the fusion protein (~50 kDa). A lower band of 30 kDa may represent a putative degradation product. Beta-tubulin was used to normalize for loading. UNTR = untransfected.

be observed in COS-1 cells, but at much lower levels compared with the WT protein at similar exposure times (fig. 6B–6D).

Human RD3-Mutation Screen

To examine whether mutations in the human *RD3* gene are associated with retinal disease, we performed mutation screening of 461 probands with retinopathy from North America (including at least 30 with cone dystrophy or CRD and 15 probands with LCA), 103 probands of Indian descent who had retinal dystrophy, 302 probands (177 with autosomal dominant RP, 96 with autosomal recessive RP, and 29 with cone dystrophy or CRD) from the United Kingdom, and 15 probands with CRD from Scandinavia. We sequenced all coding exons, including the flanking intron/exon boundaries (fig. 7A).

Of particular interest were two siblings from India who had LCA (fig. 7B). Both probands have had poor vision since birth: nystagmus and atrophic lesions in the macular area, with pigment migration. Fundus photographs of the affected siblings are shown in figure 7C. A homozygous G→A transition in the donor splice site at the end of exon 2 (c.296+1G→A) was observed in both siblings (fig. 7D). When the splice site is removed, the 99th codon still encodes arginine and is followed by a stop codon, suggesting that the protein is prematurely truncated. RFLP analysis of other family members demonstrated that the homozygous change was present only in the affected members of the family, with unaffected members heterozygous for the mutation (fig. 7E). We examined 121 unrelated ethnically matched controls by RFLP and did not observe this nucleotide substitution. The G→A alteration was not ob-

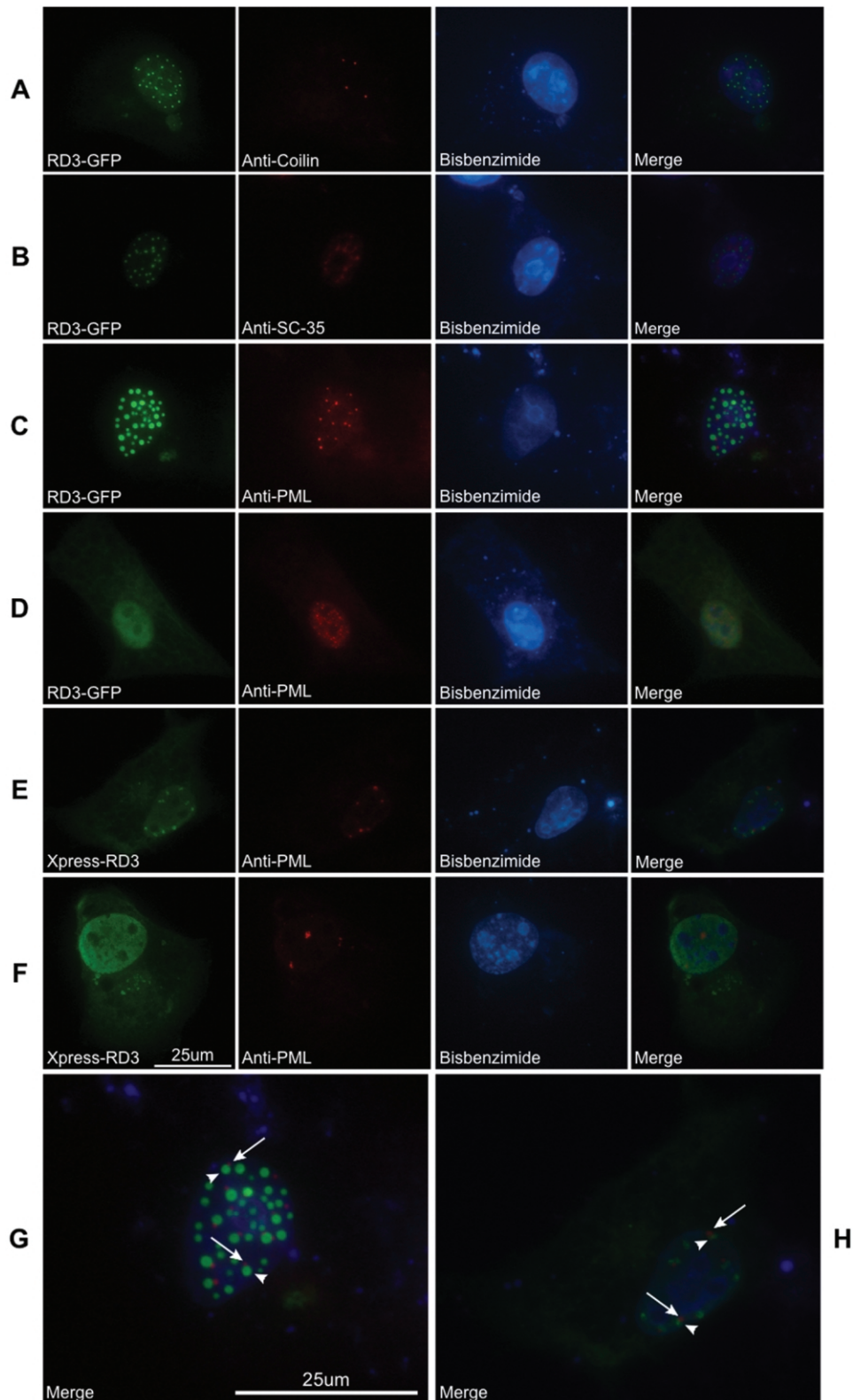


Figure 5. Immunolocalization of the RD3 protein. Mouse *Rd3* cDNA was placed in either the pEGFPN1 or the pcDNA4 vector and was expressed in COS-1 cells. The cells were observed directly via GFP or with use of an anti-Xpress antibody (*green*). Cells were also stained with subnuclear markers (*red*), to test for colocalization. Bisbenzimidide was used to stain the nuclei (*blue*). *A*, RD3-GFP and Cajal body marker anti-coilin. *B*, RD3-GFP and nuclear speckle marker anti-SC-35. *C* and *D*, RD3-GFP and PML body marker anti-PML. *E* and *F*, Xpress-RD3 and anti-PML antibody. *G* and *H*, Higher magnification of the merged images from panels *C* and *E*, respectively. Close localization of RD3 and PML bodies are marked with an arrowhead and an arrow, respectively.

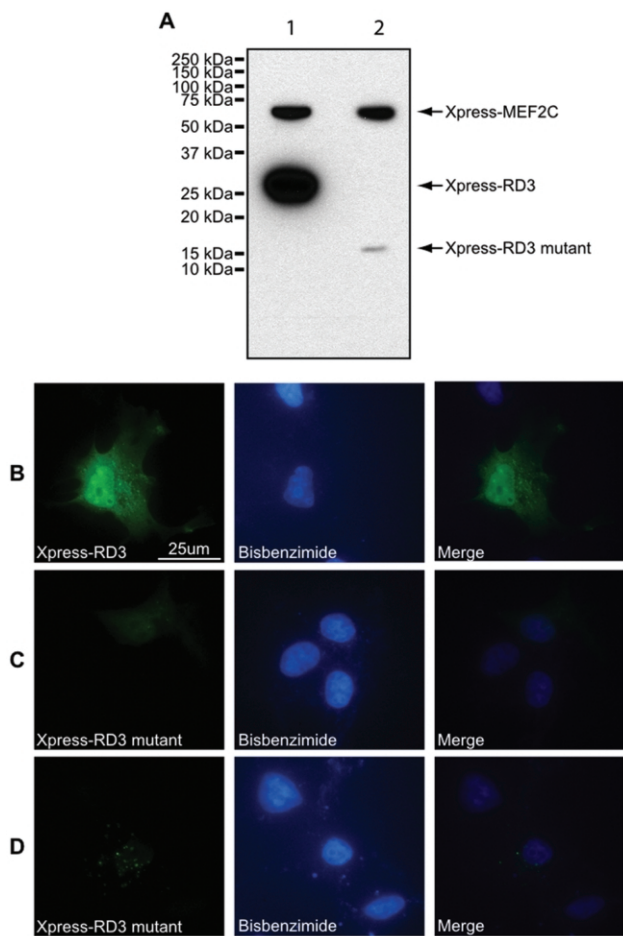


Figure 6. A, Examination of the mouse *rd3* mutation in COS-1 cells. Equal amounts of WT (lane 1) and mutant (lane 2) *Rd3*-pcDNA4 vectors were cotransfected with *Mef2c*-pcDNA4 into COS-1 cells. Cells were examined by immunoblot with use of anti-Xpress antibody. Roughly equal intensity of MEF2C signal shows that equal amounts of protein were loaded on the gel. WT RD3 protein is of expected molecular mass (~26 kDa), whereas the mutant RD3 protein is truncated (~15 kDa) and is expressed at lower levels. B, Immunolocalization of the RD3 protein in transfected cells, with use of WT *rd3*-pcDNA4 construct. Bisbenzimidazole was used to stain the nuclei (blue). C and D, Immunolocalization of the RD3 protein in transfected cells, with use of mutant *rd3*-pcDNA4 plasmid. Cells were examined as in panel B. Image exposures were performed in a consistent manner.

served in any other probands or controls from North America or Europe. To directly examine the impact of this change on RD3 transcript, we performed RT-PCR analysis of RNA from control lymphocytes, but no product could be amplified (data not shown).

Our mutation screening uncovered changes of uncertain significance in three female probands. The first affected individual (from North America) revealed four homozygous alterations (c.16T→C, 69G→C, 84G→A, and 235T→C) leading to two predicted amino acid changes (p.W6R, E23D, T28T, and L79L, respectively). She exhibited an atypical

late-onset form of RP. The second proband (also from North America) carried a heterozygous c.389A→T alteration encoding a predicted p.K130M. This girl presented in 1996, then aged 11 years, with a history of poor vision beginning at age 3 years but with no family history of eye problems or blindness. Fundus examination showed round atrophic lesions in both maculae, and there was a cellophane-like sheen and atrophy in the other regions of the posterior poles. By ERG, it was determined that she had a CRD pattern, with cone ERG b-wave amplitudes at about one-third of normal and rod ERG amplitudes at ~80% of normal levels. The third proband (from Scandinavia) had a heterozygous c.170G→T change encoding p.G57V. She had no family history of visual handicap but had visual problems since age 6 years. Her eye disorder was diagnosed by repeated full-field ERG, at ages 9 years and 19 years, as cone-rod degeneration with reduced but still-remaining rod and cone function. At age 19 years, fundus examination revealed macular changes with atrophy and spicular pigment in the midperiphery. Visual acuity was reduced to 20/200, with central scotoma in both eyes.

Several other alterations were observed in the heterozygous form, both in probands and in controls, or did not segregate with the disease in affected families; these include c.103G→A (p.G35R), c.139C→T (p.R47C), c.202C→T (p.R68W), c.500G→A (p.R167K), and c.584A→T (p.D195V). The population group and frequency of each alteration are listed in table 1.

To examine whether missense alterations observed in the human mutation screen affected subcellular localization of the RD3 protein, we generated p.W6R, p.E23D, p.K130M, and p.W6R;E23D mutations in the RD3-GFP-expression construct. These changes were selected because of their absence in normal controls and their presence in individual probands. The GFP-fused mutant RD3 proteins did not appear to have a substantive difference from the control in immunoblot analysis or in COS-1 localization (data not shown). Overall, our data suggest that *RD3* mutations represent a rare cause of retinopathy.

Discussion

RDs are a significant cause of untreatable blindness in the United States. Delineation of precise genetic defects in RDs and of cellular pathways that lead to photoreceptor-cell death are critical for developing knowledge-based design of treatment and therapies. In our continuing effort to identify retinal-disease genes, we have uncovered genetic defects in the *RD3* gene that are responsible for photoreceptor degeneration in the *rd3* mouse and some patients with retinopathies. Notably, RDs can be caused by mutations in photoreceptor-specific (such as rhodopsin, *RP1*, *CRX*, and *NRL*) or ubiquitously expressed (such as *RPGR*, *CHM*, and *PRPF31*) genes. The *RD3* gene exhibits an interesting expression profile: whereas it is preferentially (and highly) expressed in the retina and in photorecep-

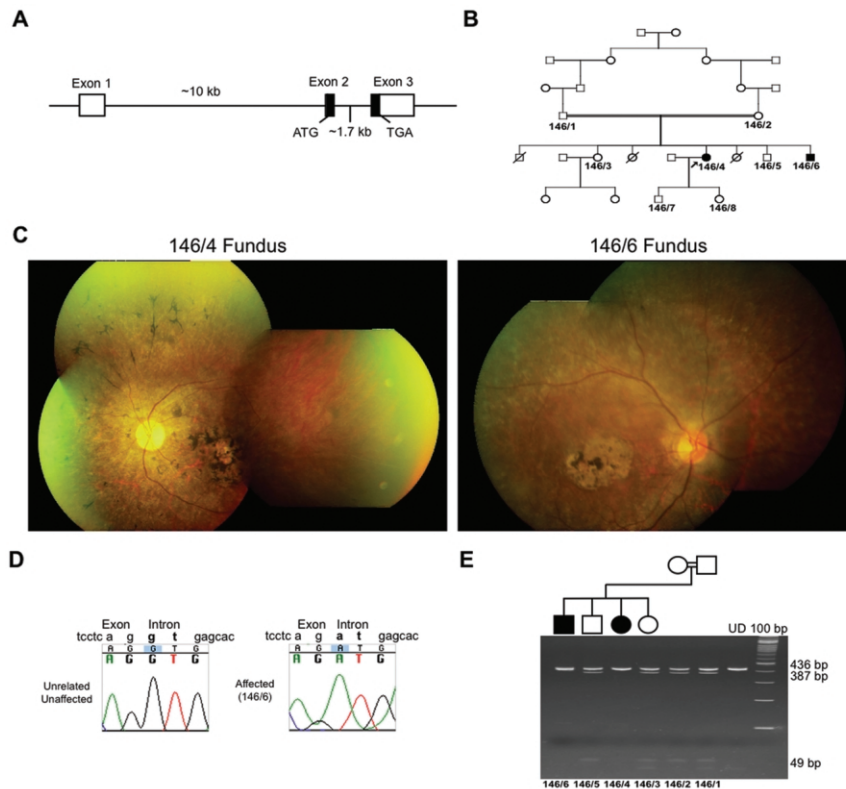


Figure 7. Findings for the LCA-affected family (from India), with a homozygous change in *RD3*. *A*, Genomic structure of the human *RD3* gene. *B*, Pedigree of family 146. Proband 146/4 is marked with an arrow. *C*, Fundus photographs of affected individuals 146/4 and 146/6. *D*, Chromatograms of unrelated unaffected subject and affected proband 146/6 at the exon2/intron2 junction. Individual 146/6 has a homozygous G→A change, which is predicted to remove the donor splice site of exon 2 and result in a stop codon after aa 99. *E*, Pedigree of a portion of family 146 and RFLP analysis of the mutation. Probands 146/4 and 146/6 show only a 436-bp band, whereas all other members show 49-bp and 387-bp bands in addition to the 436-bp band. UD = undigested.

tors, *Rd3* transcripts can be detected in mouse retinas that lack rod and cone photoreceptors.

The RD3 protein has a relatively low molecular mass (22 kDa) and includes a number of conserved sites for protein modification (specifically, phosphorylation and sumoylation). Additionally, the putative coiled-coil domain(s) might serve as protein-interaction site(s). The mutation identified in the *rd3* mouse generates a stop codon in the *Rd3* gene, thereby producing a truncated protein (of 11 kDa) that appears to be less stable, at least in transfected COS-1 cells. Hence, our data strongly implicate partial or complete loss of RD3 protein function as a possible mechanism of retinal degeneration in the *rd3* mouse. Although the *rd3* mutation is in the last exon, nonsense-mediated decay of the mutant transcript cannot be ruled out. In any event, the detection of a truncated RD3 mutant protein in COS-1 cells further validates the causal relationship of this mutation to retinopathy.

Subnuclear structures that commonly exist in cells include PML bodies, Cajal bodies, and nuclear speckles. PML bodies are implicated in diverse biological functions, including DNA repair, antiviral response, apoptosis, proteo-

lysis, gene regulation, and tumor suppression.^{33–35} PML is also suggested to be a transcriptional regulator and/or sensor of DNA damage and cellular stress.^{33–35} Cajal bodies are associated with snRNPs and snoRNPs (small nuclear and nucleolar RNAs), which are involved in pre-mRNA and rRNA processing, respectively.³⁶ Nuclear speckles are observed close to genes with highly active transcription, are linked with pre-mRNA splicing, and are suggested to form a compartment for splicing factors and proteins involved in transcription.³⁷ Interestingly, a number of retinopathy genes are associated with transcription and splicing.^{16,38–45} Varied localization of RD3 protein in COS-1 cells suggests its dynamic role in cellular processes and within subnuclear compartment(s). A reduced amount of mutant RD3 protein in transfected cells indicates that the loss of RD3 protein may compromise nuclear function(s). However, the precise role of RD3 in transcription, splicing, or other regulatory processes is subject to further experimentation.

LCA is a cause of early-onset (childhood) blindness, with an estimated prevalence of 1 in 50,000–100,000.⁴⁶ Known and putative functions and/or location of proteins encoded by mutant LCA genes are diverse and include pro-

Table 1. Summary of the RD3 Human Mutation Screen

Change	No. of Subjects with Exon Change					
	United Kingdom/ Scandinavia		India		North America	
	Proband (n = 317)	Control (n = 95)	Proband (n = 103)	Control ^a (n = 121)	Proband (n = 461)	Control (n = 175)
Homozygous c.16T→C, 69G→C, 84G→A, 235T→C (p.W6R, E23D, T28T, L79L)	0	0	0	NA	1	0
c.103G→A (p.G35R)	0	0	1	NA	0	0
c.139C→T (p.R47C)	8	2	2	NA	10	5
c.170G→T (p.G57V)	1	0	0	NA	0	0
c.202C→T (p.R68W)	0	0	1	NA	0	0
c.389A→T (p.K130M)	0	0	0	NA	1	0
c.500G→A (p.R167K)	3	0	0	NA	1	1
c.584A→T (p.D195V)	1	3	0	NA	4	6
c.296+1G→A homozygous	0	0	1 ^b	0	0	0

NOTE.—Probands with RP were sequenced for changes in exon 2 and exon 3 of *RD3*.

^a The c.296+1G→A mutation was examined in 121 Indian controls by RFLP. NA = not applicable.

^b One proband was found in the initial screen. An affected sibling was subsequently identified during follow-up.

tein trafficking, cell-cycle progression, photoreceptor morphogenesis, transcription, phototransduction, and retinoid cycle.^{4,13,18,47} *RD3* is likely responsible for a small subset of LCA, and further examination of this retinopathy might allow us to determine the proportion of *RD3* mutation-based early-onset retinopathy. We have identified two siblings carrying a mutation in the invariant G residue of the exon 2 donor splice site. Splice-site alterations are responsible for at least 15% of human mutations.⁴⁸ Mutation of the invariant G at donor splice site +1 is a commonly reported cause of human disease (Human Gene Mutation Database).⁴⁹ It is possible that a cryptic splice site within exon 2 or intron 2 is used after the invariant G is changed. Additionally, exon 2 may be skipped entirely,⁵⁰ or the mRNA may be subject to nonsense-mediated decay.⁵¹ Within exon 2, there are two potential cryptic splice sites—c.159 and c.169—with scores of 0.50 and 0.43, respectively. After the normal exon 2 splice site, the next putative splice sites are at nucleotides c.296+219 and c.296+432 (respective scores 0.41 and 1.00). The likely splicing site for mutant allele is c.296+432, because of its high score⁵² (Berkeley *Drosophila* Genome Project: Splice Site Prediction by Neural Network Web site). The splice-site mutation is predicted to result in a truncated RD3 protein, ending at aa 99. This shortened protein would be similar to the 107-aa protein in the *rd3* mice, thereby raising the possibility that the *rd3* mouse is a useful mouse model for the retinal disease in this family. Notably, the *rd3* mice exhibit a relatively quick degeneration of photoreceptors. For example, ONL loss in RBF/DnJ-*rd3/rd3* mice is complete in ~8 wk.¹⁹ In comparison, the quite severe *Pde6b*^{del} and *Rd4* mouse retinas show severe degeneration by age 1 mo and 2 mo, respectively.⁵³ Several strains of mutant mice reveal much slower photoreceptor loss than do *rd3*, with complete degeneration as late as age 30 mo.⁵³

In the one proband carrying four homozygous alterations, W6 and E23 residues are conserved in almost all species. Codon 6 in chimpanzee is arginine (instead of tryptophan), and codon 23 in frog is aspartic acid (instead of glutamic acid). Since W6R and E23D alterations exist individually in chimpanzee and frog, it is difficult to conclude whether these changes cause disease in humans. Additional work would be required to fully characterize the functional effect of these alterations. For c.389A→T (p.K130M)– and c.16T→C;69G→C;84G→A;235T→C (p.W6R; E23D;T28T;L79L)–containing probands, we attempted to collect DNA samples from the respective families but were unsuccessful. Although c.389A→T (p.K130M) and c.170G→T (p.G57V) heterozygous changes are not observed in our cohort of controls, we learned that these subjects are of Chinese and mixed European–Middle Eastern descent, respectively. Screening of ethnically matched controls might be necessary to determine whether these changes are polymorphic in their respective populations. We identified several additional nucleotide changes that do not appear to be associated with disease in heterozygous state; these are c.103G→A (p.G35R), c.139C→T (p.R47C), c.202C→T (p.R68W), c.500G→A (p.R167K), and c.584A→T (p.D195V).

Since the splice-site alteration represents the only likely disease-causing mutation in 881 examined probands, we suggest that *RD3* mutations are a rare cause of retinal disease. *C1orf36* (*RD3*) was tested elsewhere as a candidate retinal-disease gene; however, no significant alterations were observed in this earlier study.³⁰ Recently, initial screening of coding regions in patients with retinopathy did not reveal any disease-causing mutation in *CEP290/NPHP6*, and only the lymphocyte RNA analysis established it as a major LCA gene.¹⁸ However, unlike *CEP290*, *RD3* is not detected in lymphocytes.

Recent studies suggest a more dynamic environment in the nucleus than previously expected.⁵⁴ Discrete nuclear processes (such as steps in gene transcription and post-transcriptional events) appear to be mediated by association of gene regions, transcribed sequences, and/or proteins in unique subnuclear compartments. PML bodies are

but one component of the nucleus whose role(s) is not completely understood. The discovery of *RD3* and its further characterization might allow us to gain insights into fundamental regulatory events that are necessary for retinal function.

Acknowledgments

We thank Amna Shah, for technical assistance, M. N. Mandal and members of the Swaroop lab, for reagents and critical comments, and S. Ferrara, for administrative support. This work was supported in part by National Institutes of Health grants EY011115, EY007003, and EY007758 and by the Foundation Fighting Blindness, the Elmer and Silvia Sramek Foundation, and Research to Prevent Blindness. J.S.F. is a recipient of a Canadian Institutes of Health Research postdoctoral fellowship.

Web Resources

The URLs for data presented herein are as follows:

Berkeley *Drosophila* Genome Project: Splice Site Prediction by Neural Network, http://www.fruitfly.org/seq_tools/splice.html
Human Gene Mutation Database, <http://www.hgmd.org/>
NCBI Expression Profile Viewer, <http://www.ncbi.nlm.nih.gov/UniGene/ESTProfileViewer.cgi?uglist=Hs.632495> (for Hs.632495)
Online Mendelian Inheritance in Man (OMIM), <http://www.ncbi.nlm.nih.gov/Omim/> (for RP and LCA)
RetNet, <http://www.sph.uth.tmc.edu/Retnet/>

References

1. Rivolta C, Sharon D, DeAngelis MM, Dryja TP (2002) Retinitis pigmentosa and allied diseases: numerous diseases, genes, and inheritance patterns. *Hum Mol Genet* 11:1219–1227
2. Kennan A, Aherne A, Humphries P (2005) Light in retinitis pigmentosa. *Trends Genet* 21:103–110
3. Fain GL (2006) Why photoreceptors die (and why they don't). *Bioessays* 28:344–354
4. Koenekoop RK (2004) An overview of Leber congenital amaurosis: a model to understand human retinal development. *Surv Ophthalmol* 49:379–398
5. Weleber RG (2005) Inherited and orphan retinal diseases: phenotypes, genotypes, and probable treatment groups. *Retina* 25:S4–S7
6. Daiger SP (2004) Identifying retinal disease genes: how far have we come, how far do we have to go? *Novartis Found Symp* 255:17–27
7. Chang B, Hawes NL, Hurd RE, Wang J, Howell D, Davisson MT, Roderick TH, Nusinowitz S, Heckenlively JR (2005) Mouse models of ocular diseases. *Vis Neurosci* 22:587–593
8. Rakoczy EP, Yu MJ, Nusinowitz S, Chang B, Heckenlively JR (2006) Mouse models of age-related macular degeneration. *Exp Eye Res* 82:741–752
9. Bowes C, Li T, Danciger M, Baxter LC, Applebury ML, Farber DB (1990) Retinal degeneration in the rd mouse is caused by a defect in the β subunit of rod cGMP-phosphodiesterase. *Nature* 347:677–680
10. Pittler SJ, Baehr W (1991) Identification of a nonsense mutation in the rod photoreceptor cGMP phosphodiesterase beta-subunit gene of the *rd* mouse. *Proc Natl Acad Sci USA* 88:8322–8326
11. Travis GH, Brennan MB, Danielson PE, Kozak CA, Sutcliffe JG (1989) Identification of a photoreceptor-specific mRNA encoded by the gene responsible for retinal degeneration slow (*rd*s). *Nature* 338:70–73
12. Akhmedov NB, Piriev NI, Chang B, Rapoport AL, Hawes NL, Nishina PM, Nusinowitz S, Heckenlively JR, Roderick TH, Kozak CA, Danciger M, Davisson MT, Farber DB (2000) A deletion in a photoreceptor-specific nuclear receptor mRNA causes retinal degeneration in the *rd7* mouse. *Proc Natl Acad Sci USA* 97:5551–5556
13. Chang B, Khanna H, Hawes NL, Jimeno D, He S, Lillo C, Parapuram SK, Cheng H, Scott A, Hurd RE, Sayer JA, Otto EA, Attanasio M, O'Toole JF, Jin G, Shou C, Hildebrandt F, Williams DS, Heckenlively JR, Swaroop A (2006) An in-frame deletion in a novel centrosomal/ciliary protein CEP290/NPHP6 perturbs its interaction with RPGR and results in early-onset retinal degeneration in the *rd16* mouse. *Hum Mol Genet* 15:1847–1857
14. Kajiwara K, Hahn LB, Mukai S, Travis GH, Berson EL, Dryja TP (1991) Mutations in the human retinal degeneration slow gene in autosomal dominant retinitis pigmentosa. *Nature* 354:480–483
15. McLaughlin ME, Sandberg MA, Berson EL, Dryja TP (1993) Recessive mutations in the gene encoding the β -subunit of rod phosphodiesterase in patients with retinitis pigmentosa. *Nat Genet* 4:130–134
16. Haider NB, Jacobson SG, Cideciyan AV, Swiderski R, Streb LM, Searby C, Beck G, Hockey R, Hanna DB, Gorman S, Duhl D, Carmi R, Bennett J, Weleber RG, Fishman GA, Wright AF, Stone EM, Sheffield VC (2000) Mutation of a nuclear receptor gene, *NR2E3*, causes enhanced S cone syndrome, a disorder of retinal cell fate. *Nat Genet* 24:127–131
17. Sayer JA, Otto EA, O'Toole JF, Nurnberg G, Kennedy MA, Becker C, Hennies HC, et al (2006) The centrosomal protein nephrocystin-6 is mutated in Joubert syndrome and activates transcription factor ATF4. *Nat Genet* 38:674–681
18. den Hollander AI, Koenekoop RK, Yzer S, Lopez I, Arends ML, Voeseke KEJ, Zonneveld MN, Strom TM, Meitinger T, Brunner HG, Hoyng CB, van den Born LI, Rohrschneider K, Cremers FPM (2006) Mutations in the *CEP290* (*NPHP6*) gene are a frequent cause of Leber congenital amaurosis. *Am J Hum Genet* 79:556–561
19. Heckenlively JR, Chang B, Peng C, Hawes NL, Roderick TH (1993) Variable expressivity of rd-3 retinal degeneration dependent on background strain. In: Hollyfield JG, Anderson RE, LaVail MM (eds) *Retinal degeneration*. Plenum Press, New York, pp 273–280
20. Linberg KA, Fariss RN, Heckenlively JR, Farber DB, Fisher SK (2005) Morphological characterization of the retinal degeneration in three strains of mice carrying the *rd-3* mutation. *Vis Neurosci* 22:721–734
21. Danciger JS, Danciger M, Nusinowitz S, Rickabaugh T, Farber DB (1999) Genetic and physical maps of the mouse rd3 locus: exclusion of the ortholog of USH2A. *Mamm Genome* 10:657–661
22. Pieke-Dahl S, Ohlemiller KK, McGee J, Walsh EJ, Kimberling WJ (1997) Hearing loss in the RBF/Dnj mouse, a proposed animal model of Usher syndrome type IIa. *Hear Res* 112:1–12
23. Pang JJ, Chang B, Hawes NL, Hurd RE, Davisson MT, Li J, Noorwez SM, Malhotra R, McDowell JH, Kaushal S, Hauswirth WW, Nusinowitz S, Thompson DA, Heckenlively JR (2005) Retinal degeneration 12 (*rd12*): a new, spontaneously arising

- mouse model for human Leber congenital amaurosis (LCA). *Mol Vis* 11:152–162
24. Mears AJ, Kondo M, Swain PK, Takada Y, Bush RA, Saunders TL, Sieving PA, Swaroop A (2001) Nrl is required for rod photoreceptor development. *Nat Genet* 29:447–452
 25. Furukawa T, Morrow EM, Li T, Davis FC, Cepko CL (1999) Retinopathy and attenuated circadian entrainment in Crx-deficient mice. *Nat Genet* 23:466–470
 26. Friedman JS, Ducharme R, Raymond V, Walter MA (2000) Isolation of a novel iris-specific and leucine-rich repeat protein (oculoglycan) using differential selection. *Invest Ophthalmol Vis Sci* 41:2059–2066
 27. Friedman JS, Khanna H, Swain PK, Denicola R, Cheng H, Mitton KP, Weber CH, Hicks D, Swaroop A (2004) The minimal transactivation domain of the basic motif-leucine zipper transcription factor NRL interacts with TATA-binding protein. *J Biol Chem* 279:47233–47241
 28. Chang B, Heckenlively JR, Hawes NL, Roderick TH (1993) New mouse primary retinal degeneration (*rd-3*). *Genomics* 16:45–49
 29. Akimoto M, Cheng H, Zhu D, Brzezinski JA, Khanna R, Filippova E, Oh EC, Jing Y, Linares JL, Brooks M, Zarepari S, Mears AJ, Hero A, Glaser T, Swaroop A (2006) Targeting of GFP to newborn rods by Nrl promoter and temporal expression profiling of flow-sorted photoreceptors. *Proc Natl Acad Sci USA* 103:3890–3895
 30. Lavorgna G, Lestingi M, Ziviello C, Testa F, Simonelli F, Manitto MP, Brancato R, Ferrari M, Rinaldi E, Ciccodicola A, Banfi S (2003) Identification and characterization of *C1orf36*, a transcript highly expressed in photoreceptor cells, and mutation analysis in retinitis pigmentosa. *Biochem Biophys Res Commun* 308:414–421
 31. Blackshaw S, Fraioli RE, Furukawa T, Cepko CL (2001) Comprehensive analysis of photoreceptor gene expression and the identification of candidate retinal disease genes. *Cell* 107:579–589
 32. Lupas A, Van Dyke M, Stock J (1991) Predicting coiled coils from protein sequences. *Science* 252:1162–1164
 33. Zhong S, Salomoni P, Pandolfi PP (2000) The transcriptional role of PML and the nuclear body. *Nat Cell Biol* 2:E85–90
 34. Strudwick S, Borden KL (2002) Finding a role for PML in APL pathogenesis: a critical assessment of potential PML activities. *Leukemia* 16:1906–1917
 35. Dellaire G, Bazett-Jones DP (2004) PML nuclear bodies: dynamic sensors of DNA damage and cellular stress. *Bioessays* 26:963–977
 36. Cioce M, Lamond AI (2005) Cajal bodies: a long history of discovery. *Annu Rev Cell Dev Biol* 21:105–131
 37. Lamond AI, Spector DL (2003) Nuclear speckles: a model for nuclear organelles. *Nat Rev Mol Cell Biol* 4:605–612
 38. Bessant DA, Payne AM, Mitton KP, Wang QL, Swain PK, Plant C, Bird AC, Zack DJ, Swaroop A, Bhattacharya SS (1999) A mutation in NRL is associated with autosomal dominant retinitis pigmentosa. *Nat Genet* 21:355–356
 39. Sohocki MM, Sullivan LS, Mintz-Hittner HA, Birch D, Heckenlively JR, Freund CL, McInnes RR, Daiger SP (1998) A range of clinical phenotypes associated with mutations in *CRX*, a photoreceptor transcription-factor gene. *Am J Hum Genet* 63:1307–1315
 40. Banerjee P, Kley PW, Knowles JA, Lewis CA, Ross BM, Parano E, Kovats SG, Lee JJ, Penchaszadeh GK, Ott J, Jacobson SG, Gilliam TC (1998) *TULP1* mutation in two extended Dominican kindreds with autosomal recessive retinitis pigmentosa. *Nat Genet* 18:177–179
 41. Boggon TJ, Shan WS, Santagata S, Myers SC, Shapiro L (1999) Implication of tubby proteins as transcription factors by structure-based functional analysis. *Science* 286:2119–2125
 42. McKie AB, McHale JC, Keen TJ, Tarttelin EE, Goliath R, van Lith-Verhoeven JJ, Greenberg J, Ramesar RS, Hoyng CB, Cremers FP, Mackey DA, Bhattacharya SS, Bird AC, Markham AF, Inglehearn CF (2001) Mutations in the pre-mRNA splicing factor gene *PRPC8* in autosomal dominant retinitis pigmentosa (RP13). *Hum Mol Genet* 10:1555–1562
 43. Vithana EN, Abu-Safieh L, Allen MJ, Carey A, Papaioannou M, Chakarova C, Al-Magthteh M, Ebenezer ND, Willis C, Moore AT, Bird AC, Hunt DM, Bhattacharya SS (2001) A human homolog of yeast pre-mRNA splicing gene, *PRP31*, underlies autosomal dominant retinitis pigmentosa on chromosome 19q13.4 (*RP11*). *Mol Cell* 8:375–381
 44. Chakarova CF, Hims MM, Bolz H, Abu-Safieh L, Patel RJ, Papaioannou MG, Inglehearn CF, Keen TJ, Willis C, Moore AT, Rosenberg T, Webster AR, Bird AC, Gal A, Hunt D, Vithana EN, Bhattacharya SS (2002) Mutations in *HPRP3*, a third member of pre-mRNA splicing factor genes, implicated in autosomal dominant retinitis pigmentosa. *Hum Mol Genet* 11:87–92
 45. Keen TJ, Hims MM, McKie AB, Moore AT, Doran RM, Mackey DA, Mansfield DC, Mueller RF, Bhattacharya SS, Bird AC, Markham AF, Inglehearn CF (2002) Mutations in a protein target of the Pim-1 kinase associated with the RP9 form of autosomal dominant retinitis pigmentosa. *Eur J Hum Genet* 10:245–249
 46. Allikmets R (2004) Leber congenital amaurosis: a genetic paradigm. *Ophthalmic Genet* 25:67–79
 47. Janecke AR, Thompson DA, Utermann G, Becker C, Hubner CA, Schmid E, McHenry CL, Nair AR, Ruschendorf F, Heckenlively J, Wissinger B, Nurnberg P, Gal A (2004) Mutations in *RDH12* encoding a photoreceptor cell retinol dehydrogenase cause childhood-onset severe retinal dystrophy. *Nat Genet* 36:850–854
 48. Krawczak M, Reiss J, Cooper DN (1992) The mutational spectrum of single base-pair substitutions in mRNA splice junctions of human genes: causes and consequences. *Hum Genet* 90:41–54
 49. Stenson PD, Ball EV, Mort M, Phillips AD, Shiel JA, Thomas NS, Abeyasinghe S, Krawczak M, Cooper DN (2003) Human Gene Mutation Database (HGMD): 2003 update. *Hum Mutat* 21:577–581
 50. Nakai K, Sakamoto H (1994) Construction of a novel database containing aberrant splicing mutations of mammalian genes. *Gene* 141:171–177
 51. Baker KE, Parker R (2004) Nonsense-mediated mRNA decay: terminating erroneous gene expression. *Curr Opin Cell Biol* 16:293–299
 52. Reese MG, Eeckman FH, Kulp D, Haussler D (1997) Improved splice site detection in Genie. *J Comput Biol* 4:311–323
 53. Chang B, Hawes NL, Hurd RE, Davisson MT, Nusinowitz S, Heckenlively JR (2002) Retinal degeneration mutants in the mouse. *Vision Res* 42:517–525
 54. Akhtar A, Matera AG (2006) In and around the nucleus. *Nat Cell Biol* 8:3–6